Engineering Chemistry
ISSN: 2813-6535, Vol. 2, pp 13-22
doi:10.4028/p-91j5nn

Submitted: 2022-12-25
Revised: 2023-02-21
Accepted: 2023-02-21
Online: 2023-05-16

Study of Temperature Effect on the Structure and Optical Properties of RIT- 62 Cu-MOFs

Vinuta Kamat[1,a], Vinayak Adimule[2,b], Basappa C Yallur[3,c*], Manjunath D.H.[4,d*], Sheetal Batakurki[5,e**]

[1]Department of Chemistry, Mangalore University, Mangalore-574199, Karnataka.

[2]Angadi Institute of Technology and Management (AITM), Savagaon Road, Belagavi 591108. Karnataka, India.

[3]Department of Chemistry, M.S. Ramaiah Institute of Technology (Affiliated to VTU), Bangalore-560054, Karnataka, India.

[4]Department of studies in Chemistry, Shivagangothri, Davangere University, Davangere - 577 007, India.

[5]Department of Chemistry M. S. Ramaiah University of Applied Sciences, Bangalore-560054, Karnataka, India.

[a]vinutakamat24@gmail.com, [b]adimulevinayak@yahoo.in, [c*]yallurbc@gmail.com, [d]manjunathdh@davangereuniversity.ac.in, [e**]sheetalrb@gmail.com.

Keywords: MOFs, Copper composites, RIT-62 Cu-MOFs, Nano metal oxide, Optical properties.

Abstract. Metal organic frameworks are the materials of today's generation and are widely used for their various physicochemical properties. MOFs are synthesized by various methods such chemical precipitation method, sol-gel method, hydrothermal method etc. To attain the required optoelectronic properties of MOFs, synthetic methods play a important role. In the present work, the synthesis of Cu-MOFs was carried out at 80 °C and 120 °C. The synthesized Cu-MOFs were labeled as RIT 62-Cu-MOF-1 and RIT 62-Cu-MOF-2. Both the Cu-MOFs were characterized by FTIR, UV-visible spectra. The FESEM of both Cu-MOFs indicated that spherical particles with 120 to 200 nms. of particle size. Tauc's method was employed to compute the band gap of both Cu-MOFs. RIT 62-Cu-MOF-1 imparted 2.67 eV while RIT 62-Cu-MOF-2 imparted average of 2.06 eV off bandgap. 2.35 eV due to ligand-metal charge transfer observed through UV- visible spectra. Further, optimization of synthetic procedures to enhance the optical properties of Cu-MOFs.

Introduction

The filed "optoelectronics" deals with the study of interaction of electromagnetic light with the materials of interest. Various metal-based materials are synthesized to achieve the high conducting nature for varied applications such as semiconductors, optical fibers in electronic field, biosensing and bio-imaging in medical filed, solar energy devices an efficient light source, both photocatalysis and electrocatalysis in bioremediation of dyes and drugs, as a non-invasive technique in determination of heavy metals, hazardous elements in agricultural crops, etc., [1]. Reflectivity, refractivity, transparency, translucent, opaque, thermal emission, photoconductivity, luminescence, absorptivity, optical activity, scattering, turbidity, fluorescence and phosphorescence, birefringence, etc., are all the properties of optical active material [2-7]. The optical properties of the materials are significantly dependent on various factors such as particle size, thickness, composition of substance, ratio of conducting substance, structure of the material, dielectric constant etc., accounting to internal properties and external properties such as humidity, light, temperature, and wavelength of light and angle of illumination [8]. In recent years more than one metal is added as dopants to enhance the conducting nature of the materials. Transition metals and their metal oxides are believed to enhance the optoelectronic properties of the materials and are widely used as dopants [9-18]. In fact, the size reduction of metals into nanometallic form have enormously increased the physico-chemical properties of the materials [19]. Metals such as cobalt, antimony, zirconium, gadolinium, strontium,

yttrium, palladium, molybdenum, titanium, cadmium etc., have enhanced the conducting, chemical, magnetic, thermal, electronic properties of the metals and used widely for their photovoltaic applications, photoluminescence, perovskite, photocatalytic degradation, semiconductors, organic reactions etc. [20-32]. Even the small heterocyclic compounds, polymers having greater number of conjugation and easily accessible free electrons present in the heteroatoms aids in enhancing the optical properties and biological activities off the materials [33-39]. In recent years, the application of hybrid materials such as organic metal frame works have also resulted in significant contribution towards increasing the optoelectronic properties of the material [40]. Various organic linkers containing functional groups such as carboxylic acid, amine functionality, sulfur are used along with the transition metals to fine tune the required optical energy for the requisite applications [41-42]. Similarly, various metals containing iron, copper, cobalt, chromium, cadmium, vanadium, zinc, nickel, manganese, scandium, etc., along with organic framework have been reported [44]. Copper based metal organic framework having band gap energy of 2.54 eV, 2.33 eV, and 2.56 eV were obtained for the copper based with organic linkers as 1,4-benzene dicarboxylic acid, 2-amino-1,4-benzene dicarboxylic acid, and benzene-1,3,5-tricarboxylic acid synthesized by ultrasonication method and were used to trap the H_2S gas at room temperature [45]. Similarly, 1,3,5-benzenetricarboxylic acid with copper metal synthesized by the hydrothermal method reported to possess 3.86 eV band gap energy was used in photocatalytic degradation of rhodamine B dye present in the water sample [46]. Synthesis of the material plays a crucial role in attaining the required optical property of the material. Precipitations, Co-precipitation, hydrothermal method, sol–gel method, micro-emulsion, chemical- vapor deposition, electrochemical method of deposition etc., are all well reported methods in the literature for the synthesis of metal organic frame works to obtain the required optical properties. Apart from conventional heating, ultrasound and microwave heating are all employed in the synthesis of MOFs to obtain uniform crystal size, regular shape, thin films, membranes, and various other shapes are reported in the literature. Variation in temperature, stoichiometric ration of starting materials, solvent ratio, pressure, stirring time, speed, pH of the reaction etc., [47], are important parameters that aid in acquiring the requisite morphology of MOFs. In direct precipitation method, the synthesis of MOFs is carried at room temperature in presence of greener solvents [48]. The present work focuses on the investigation of temperature effect on the synthesis of copper-based MOF. The synthesized Cu MOFs are characterized by UV- Visible spectrum, FTIR and XRD. The optical properties of the MOFs are also studied.

Experimental

Materials: All the chemicals and reagents procured from Avra Synthesis Private Ltd, Sd-Fine Chemical Ltd., Sigma Aldrich, India and used without any further purifications. 1,1,3,3-tetramethoxy propane 99 % (Sigma Aldrich), 4-Mercaptobenzoic acid 99 % (Sigma Aldrich), Cu (NO3)2.3H2O 98 % (Sigma-Aldrich Ltd).

Preparation of 2-bromomalonaldehyde: Starting material 2-bromomalonaldehyde was prepared using the procedure given in literature. To a 100 ml of aqueous solution of 1, 1, 3, 3-tetramethoxypropane (100g, 0.12M), concentrated HCl (4.3mL) was added and stirred until it forms homogeneous solution, wherein temperature of the reaction mixture was maintained below 35 °C and later bromine (0.15M) solution was added drop wise slowly and stirring was continued for another 30 minutes. Then, reaction mixture was concentrated under vacuum maintaining temperature below 50 °C until thick slurry was obtained, and further washed using 200 mL cold water, 100 ml of cold dichloromethane and dried in vacuum. Yield: 65%, MP: 148 °C (Lit: 148 °C).

General Procedure for Synthesis of 4-((1,3-dioxopropan-2-yl)thio)benzoic acid (RIT 62): Mixed both 4-mercaptobenzoic acid (0.250 g, 0.0016 mol) and 2-bromomalonaldehyde (0.245 g, 0.0016 mol) in a 4 ml glass vail and did the microwave irradiation using domes- tic microwave own at high power for 2 min. Completion of the reaction was monitored by TLC and crude product was purified by column chromatography on silica gel using ethyl acetate/n-hexane (1:2) and yield is 75% (0.272 g).

Synthesis of Cu-MOF's: Cu-MOF synthesized through solvothermal method in which an equimolar amount of RIT-62 and Cu (NO3)2.3H2O were collected in DMF and kept at 80 °C and 120 °C in an oven for 48 hours. Centrifuged the reaction mixture (7000rpm for 5 min) by repeatedly washing the composite formed with DMF, then with ethanol and dried the composite in vacuum oven at 1500C.

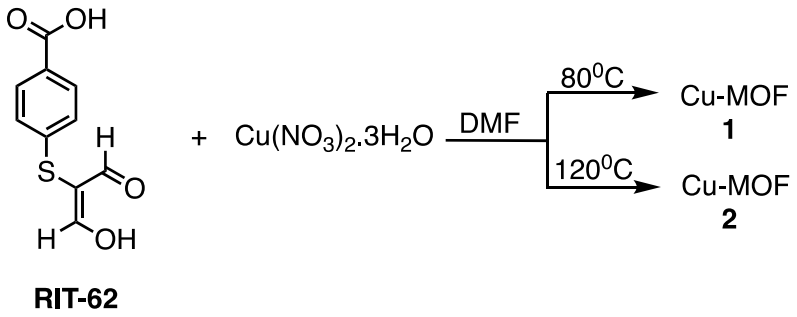

Figure 1. Preparation of Cu-MOF's: compound 1 and 2.

Result and Discussion

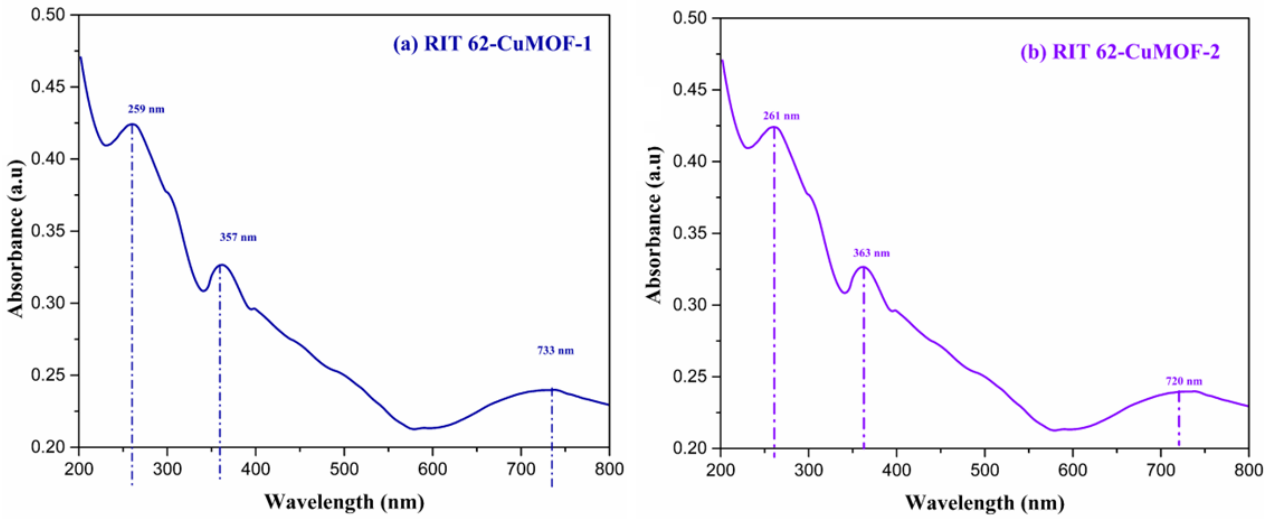

Figure 2. UV-visible spectra of (a) RIT 62-Cu-MOF-1 and (b) RIT 62-Cu-MOF-2

UV-Visible Spectral studies: The UV-Visible spectrum of the Cu-MOFs are shown in Fig No.2. The RIT 62-Cu-MOF-1 showed three characteristic bands at 259 nm, 357 nm and 733 nm. There was a slight increase in the wavelength of RIT 62-Cu-MOF-2 that showed bands at 261 nm, 363 nm whereas a decreased band at 720 nm. It is evident from the graph that there was not much temperature effect on the absorption spectrum of both Cu-MOFs. Further increase in the temperature while synthesis of Cu-MOF was avoided due to the possibility of breakage of linker which is organic molecule. Hence only two different temperatures were monitored during the synthesis. [49].

FT-IR Spectral Analysis: Figure 3. inferes the FTIR spectrum of the both Cu-MOFs. In RIT 62-Cu-MOF-1, a broad for O-H str band was observed at 3422 cm^{-1} , where as a fermi resoance band at 2917 cm^{-1} was observed for the aldehyde C-H str along with a band at 1657 cm-1, a decreased wavenumber for the aldehyde C=O streching due to the co-ordiantion band between the aldehyde carbonyl group and the copper metal oxide. Alkene C-H str was observed at 2977 cm-1. A similar peaks were observed in RIT 62-Cu-MOF-2.

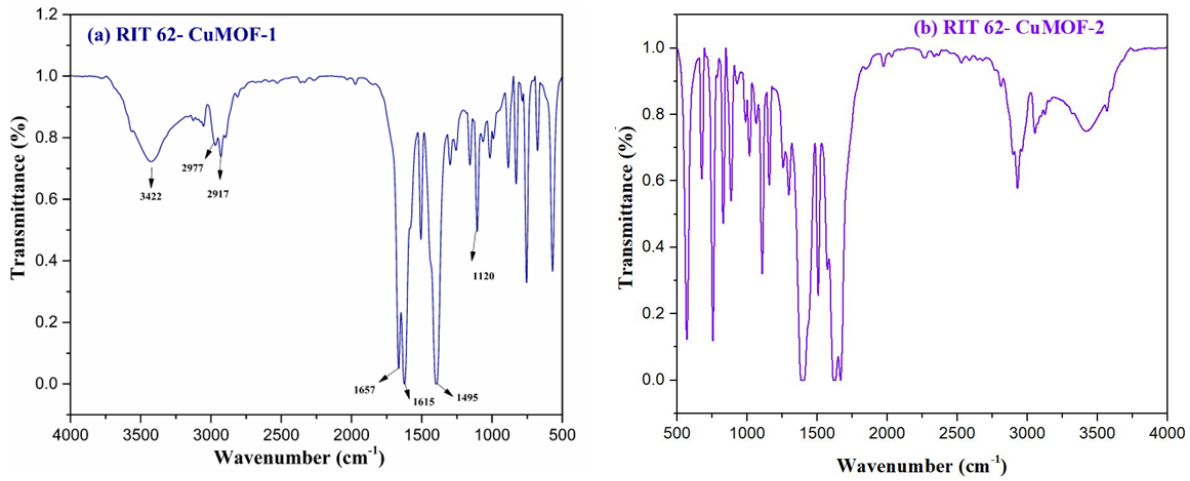

Figure 3. FTIR spectrum of RIT 62-Cu-MOF-1 and RIT 62-Cu-MOF-2

XRD diffraction studies: The X-ray diffraction studies of RIT 62-Cu-MOF-1 and RIT 62-Cu-MOF-2 were analyzed on a Bruker, Germany, fitted with D8-fine focus ceramic X-ray tube, Cu-Kα source radiation (λ =1.5406 Å) at room temperature and the graphs are depicted in the Fig. 3. The RIT 62-Cu-MOF-1 showed peaks at 2θ values of 10.18°, 12.07°, 17.3°, 26.8°, 36.80 °, 40.32°, 42.57° and 51.05° corresponding to the crystal planes at 015, 020, 032, 040, 102, 014, and 023 respectively which are in agreeable to the literature (JCPDS card number 76–1393) For RIT 62-Cu-MOF-2 the 2θ values were observed at 17.3°, 36.8 °, 40.32°, corresponding to crystal plane at 020, 032, 102, respectively. The peak intensity increased in the RIT 62-Cu-MOF-2. However, many short shoulder peaks were absent I the RIT 62-Cu-MOF-2 in comparison to RIT 62-Cu-MOF-1. The crystallite size of RIT 62-Cu-MOF-1 and RIT 62-Cu-MOF-2 were calculated using Scherrer equation and were of 150 nm, 180 nm, 250 nm respectively [51, 59, 60].

$$D = \frac{k\lambda}{\beta Cos\theta} \quad \text{---------- (1)}$$

where K is crystallite shape constant (0.94), β is full width at half maximum, λ is wavelength of X-ray Cu-Kα radiation (1.5406 Å) and θ is glancing angle.

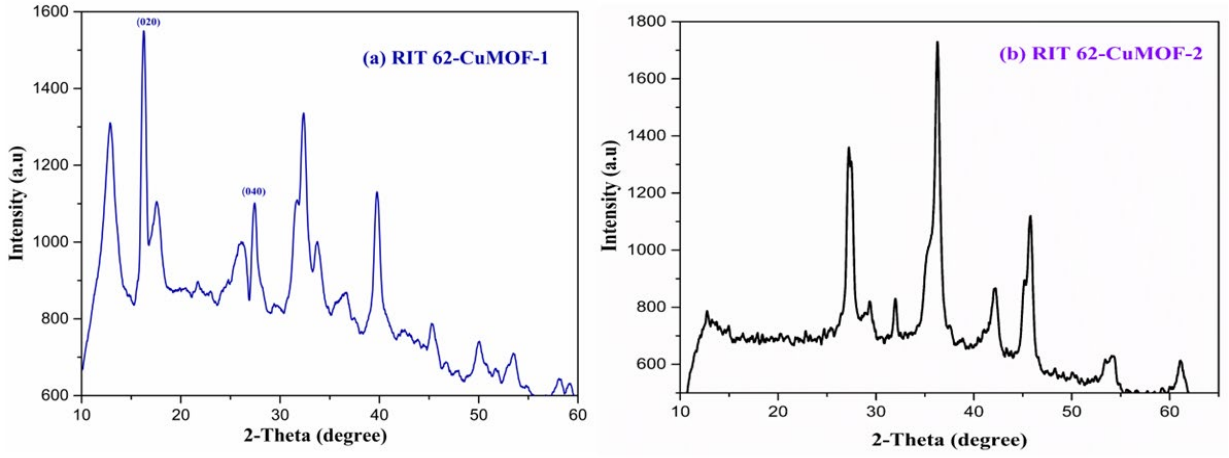

Figure 4. XRD patterns of of RIT 62-Cu-MOF-1 and RIT 62-Cu-MOF-2

The surface morphology of the RIT 62-Cu-MOF-1 and RIT 62-Cu-MOF-2 are shown in Fig no 5. The FESEM images of RIT 62-Cu-MOF-1 showed rough surface with round shape with average particle size between 150 nm to 200 nm. RIT 62-Cu-MOF-2 showed particle size between 120 nm to 200 nm. Both the images had non uniform particle size unevenly distributed throughout the surface.

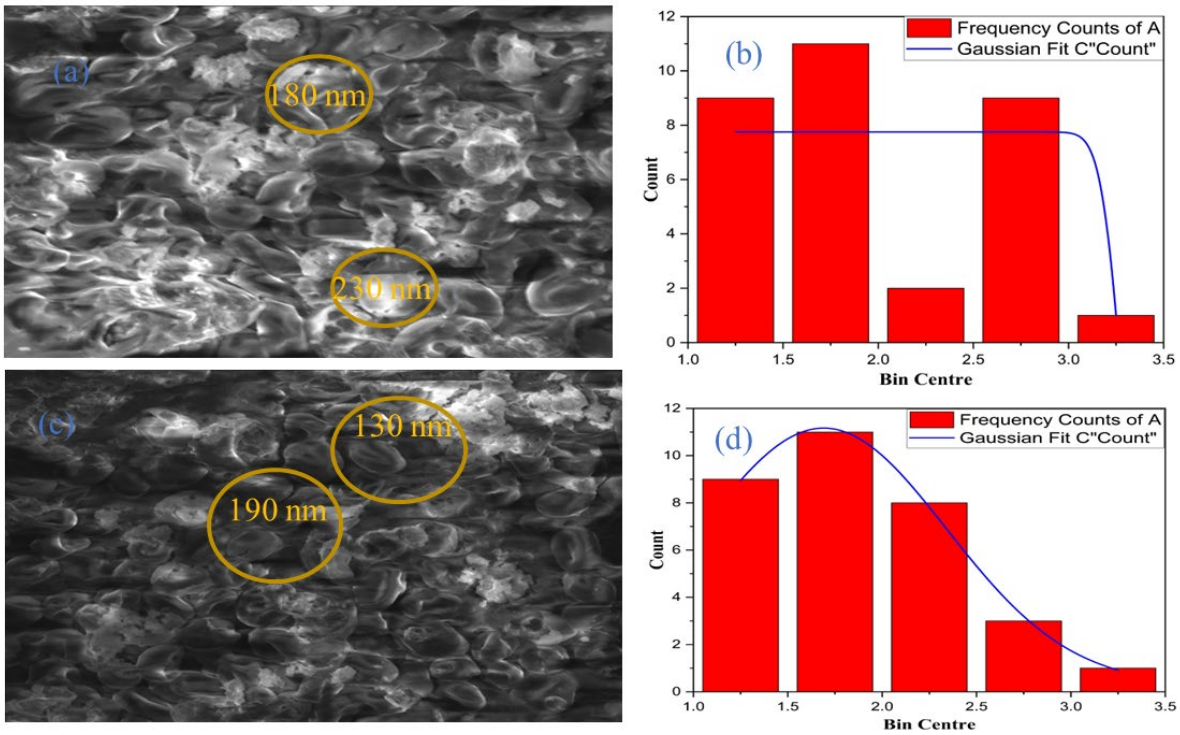

Figure 5. FESEM images (a) RIT 62-Cu-MOF-1 (b) RIT 62-Cu-MOF-2 and histograms (a) RIT 62-Cu-MOF-1, (b) RIT 62-Cu-MOF-2

Photoluminescence: Photoluminescent characteristics of Cu-MOFs are depicted in Fig. No. 6. A strong sharp absorption peak at 5-5 nm and 506 nm were observed for RIT 62-Cu-MOF-1 and RIT 62-Cu-MOF-2 respectively. A short bump was observed at 757 nm for both Cu-MOFs. Overall, there was no much difference in the PL spectra of both Cu MOFs.

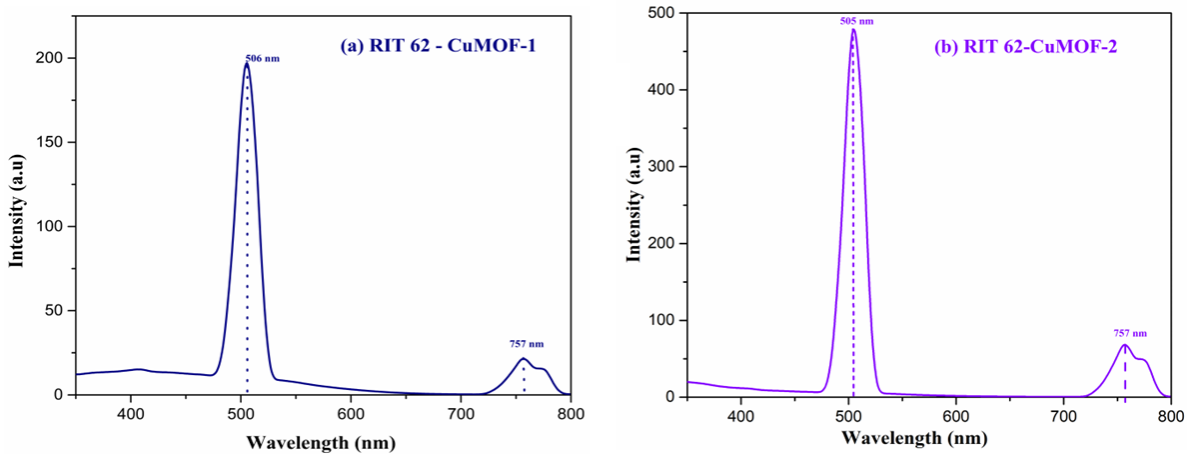

Figure 6. Photoluminescence spectra of (a) RIT 62-Cu-MOF-1 (b) RIT 62-Cu-MOF-2

Optical properties: Band gap analysis: The UV-Visible absorption spectra were recorded using 210 plus UV-Visible absorption Spectrometer. Further, bandgap energy was calculated by Tauc's method. The graph was obtained by plotting hυ (eV) versus $(\alpha h\upsilon)^2$ (eV/cm)2. The band gap energy is obtained upon extrapolating the tangential line intersecting x axis at hυ = Eg. RIT 62-Cu-MOF-1 showed the band gap energy of 2.76 eV whereas RIT 62-Cu-MOF-2 showed average band 2.03 eV. This indicates that RIT 62-Cu-MOF-2 showed better optical property compared to RIT 62-Cu-MOF-1. A slight change in their individual band gaps or lattice distortion hybridization results in shifting of the energy level [50, 51].

$$(\alpha h\nu) = A(h\gamma - E_g)^{1/2} \quad \text{---------- (2)}$$

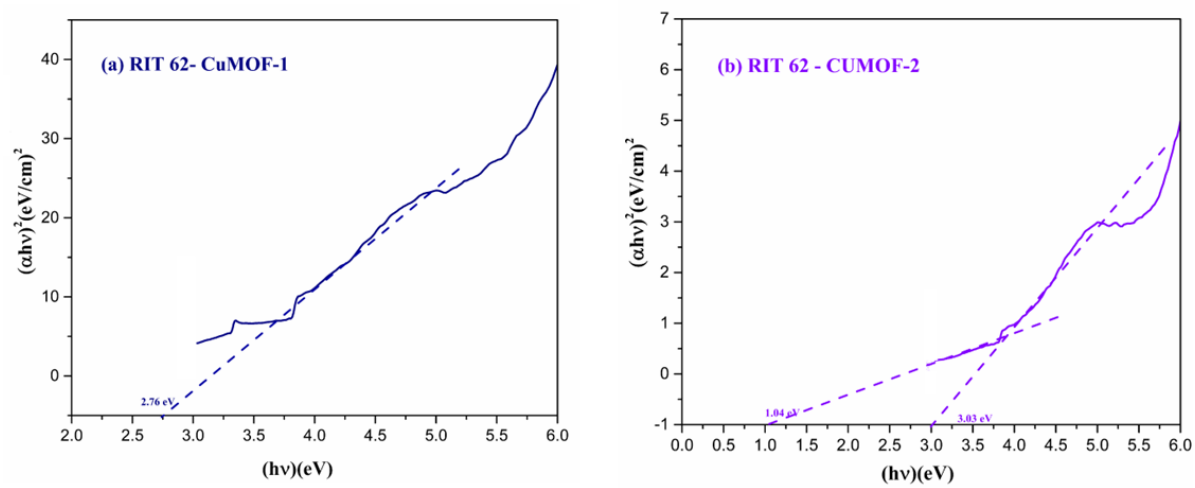

Figure 7. The energy band gaps of (a) RIT 62-Cu-MOF-1 (b) RIT 62-Cu-MOF-2

Figure 7 indicates the Tauc plots of the RIT 62-Cu-MOF-1 and RIT 62-Cu-MOF-2. RIT 62-Cu-MOF-1 showed the band gap energy of 2.76 eV whereas RIT 62-Cu-MOF-2 showed average band 2.03 eV. This indicates that RIT 62-Cu-MOF-2 showed better optical property compared to RIT 62-Cu-MOF-1.

Conclusion

The focus of this work was to investigate the temperature effect employed during the synthesis of Cu-MOF and its effect on the optical properties of the Cu-MOFs. CU-MOFs were synthesized at two different temperatures at 80 °C and 120 °C. The synthesized Cu-MOFs were characterized by UV-visible spectra, FTIR and XRD. The XRD results infer that there was slight increase in the intensity of RIT 62-Cu-MOF-2. However, both cu-MOFs showed similar particle size between 150 to 25o nm with spherical shape randomly distributed on the surface. The Pl of RIT 62-Cu-MOF-1 and RIT 62-Cu-MOF-2 showed a strong peak at 505 nm. The bandgap energy of RIT- 62-Cu-MOF-2 showed better optical property with average band gap energy as 2.03 eV when compared to the RIT 62-Cu-MOF-1 observed with bandgap energy at 2. 76 eV. Thus, Temperature parameters play an important role in obtaining narrow band gap energy. However, in this work only temperature of 80 °C to 120 °C, further increase in temperature was avoided as the change of organic linker to decompose is high. Future studies include the study of other parameters such a solvent, solvent ration, stirring time etc., to enhance the optical properties of Cu-MOFS.

References

[1] Dhand, Chetna, Neeraj Dwivedi, Xian Jun Loh, Alice Ng Jie Ying, Navin Kumar Verma, Roger W. Beuerman, Rajamani Lakshminarayanan, and Seeram Ramakrishna. Methods and strategies for the synthesis of diverse nanoparticles and their applications: a comprehensive overview. Rsc Advances. 5.127 (2015) 105003-105037.

[2] Grossweiner, Leonard I. Photophysics. The science of photobiology. (1989) 1-45.

[3] Adimule, Vinayak, Basappa C. Yallur, Sheetal R. Batakurki, and Adarsha Haramballi Jagadeesha Gowda. Microwave Assisted Synthesis of Cr doped Gd2O3 Nanostructures and Investigation on Morphology, Optical, Photoluminescence Properties. Nanoscience and Technology: An International Journal.

[4] Adimule V., S.S. Nandi, B.C. Yallur, D. Bhowmik, and A.H. Jagadeesha. Enhanced photoluminescence properties of Gd (x-1) Sr x O: CdO nanocores and their study of optical, structural, and morphological characteristics. Materials Today Chemistry. 20 (2021) 100438.

[5] Adimule Vinayak, Basappa C. Yallur, Debdas Bhowmik, and Adarsha HJ Gowda. Dielectric properties of P3BT doped ZrY2O3/CoZrY2O3 nanostructures for low-cost optoelectronics applications. Transactions on Electrical and Electronic Materials. (2021) 1-16

[6] Challa Maalathi, Basappa C. Yallur, M. R. Ambika, and Vinayak Adimule. Influence of Nano Particles on Optical Properties of Cu-MOFs. Advanced Materials Research. 1173 (2022) 23-33.

[7] Maya Pai M., Sheetal R. Batakurki, Vinayak Adimule, and Basappa C. Yallur. Optical Graphene for Biosensor Application: A Review. Applied Mechanics and Materials. 908 (2022) 51-68.

[8] Tilley, Richard JD. Colour and the optical properties of materials: an exploration of the relationship between light, the optical properties of materials and colour. John Wiley & Sons, 2010.

[9] Adimule, Vinayak, Basappa C. Yallur, Malathi Challa, and Rajeev S. Joshi. Synthesis of hierarchical structured Gd doped α-Sb2O4 as an advanced nanomaterial for high performance energy storage devices. Heliyon. 12 (2021) e08541

[10] Adimule, Vinayak, Santosh S. Nandi, B. C. Yallur, Debdas Bhowmik, and Adarsha Haramballi Jagadeesha. Optical, Structural and Photoluminescence Properties of Gd x SrO: CdO Nanostructures Synthesized by Co Precipitation Method. Journal of Fluorescence. 31, 2 (2021) 487-499.

[11] Adimule, Vinayak, B. C. Yallur, Debdas Bhowmik, and Adarsha Haramballi Jagadeesha Gowda. Morphology, structural and photoluminescence properties of shaping triple semiconductor Y x CoO: ZrO 2 nanostructures. Journal of Materials Science: Materials in Electronics. 32, 9 (2021) 12164-12181.

[12] Adimule, Vinayak, Santosh S. Nandi, B. C. Yallur, and Nilophar Shaikh. CNT/graphene-assisted flexible thin-film preparation for stretchable electronics and superconductors. Sensors for Stretchable Electronics in Nanotechnology. (2021) 89-103.

[13] Nandi, Santosh S., Anusha Suryavanshi, Vinayak Adimule, and Basappa C. Yallur. Fabrication of novel rare earth doped ionic perovskite nanomaterials of Sr0. 5, Cu0. 4, Y0. 1 and Sr0. 5 and Mn0. 5 for high power efficient energy harvesting photovoltaic cells. AIP Conference Proceedings. 2274, 1 (2020) 020005.

[14] Adimule, Vinayak, Anusha Suryavanshi, Yallur BC, and Santosh S. Nandi. A Facile Synthesis of Poly (3-octyl thiophene): Ni0. 4Sr0. 6TiO3 Hybrid Nanocomposites for Solar Cell Applications. Macromolecular Symposia. 392, 1 (2020) 2000001.

[15] Adimule V., Yallur B. C, Gowda, A. (2022). 'Crystal Structure, Morphology, Optical and Super-Capacitor Properties of Srx: α-Sb2O4 Nanostructures. Analytical and Bioanalytical Electrochemistry. 14, 1 (2022) 1-17.

[16] Adimule V, Yallur B.C., Batakurki S. R., Nandi S. S. Synthesis, Morphology and Enhanced Optical Properties of Novel GdxCo3O4 Nanostructures. Advanced Materials Research 1173 (2022) 71–82.

[17] Adimule V., Batakurki S., Yallur B. C. Enhanced photoluminescence, optical, structural properties of ZrO_2-incorporated Sm_2O_3:Co_3O_4 nanocomposite and their applications in photocatalytic degradation of methylene blue. Journal of Materials Research. 37 (2022) 2396–2405.

[18] Vinayak Adimule, Vinay S. Bhat, Basappa C. Yallur, Adarsha H. J. Gowda, Paola De Padova, Gurumurthy Hegde and Arafat Toghan. Facile synthesis of novel SrO 0.5:MnO 0.5 bimetallic oxide nanostructure as a high- performance electrode material for supercapacitors. Nanomaterials and Nanotechnology. 12 (2022) 1-14

[19] a)R. Shashanka, Effect of Sintering Temperature on the Pitting Corrosion of Ball Milled Duplex Stainless Steel by using Linear Sweep Voltammetry. Anal. Bioanal. Electrochem. 10 (2018) 349-361. b). Pokropivny, V., Lohmus, R., Hussainova, I., Pokropivny, A., & Vlassov, S. Introduction to nanomaterials and nanotechnology. Vol. 1. Ukraine: Tartu University Press, 2007.

[20] Nandi S. S., Adimule V., and Yallur B. C. (2022). Synthesis, Structural and Optical Properties of Co Doped Sm2O3 Nanostructures. In Advanced Materials Research. 1173 (2022) 59–69.

[21] Adimule V., Batakurki S., Yallur B. C. Samarium-decorated ZrO_2@SnO_2 nanostructures, their electrical, optical and enhanced photoluminescence properties. J Mater Sci: Mater. Electron. 33, (2022) 18699–18715.

[22] Malathi Challa, M. R. Ambika, S. R. Usharani, Basappa C. Yallur, Vinayak Adimule. Enhancement of Band Gap Energy and Crystallinity of Cu-MOFs Due to Doping of Nano Metal Oxide. Advanced Materials Research. 1173 (2022) 13-22.

[23] Malathi Challa, Ambika M.R, Usharani S.R, Sheetal Batakurki, Basappa C. Yallur. Modulation of Optical Band Gap of 2-Amino Terephthalic Acid Cu-MOFs Doped with Ag2O and rGO. Advanced Materials Research. 1173 (2022) 35-45. https://doi.org/10.4028/p-i3rcg6.

[24] Vinayak Adimule, Basappa C. Yallur, Sheetal R. Batakurki, Santosh S. Nandi. Synthesis, Morphology and Enhanced Optical Properties of Novel GdxCo_3O_4 Nanostructures. Advanced Materials Research. 1173 (2022) 71-82.

[25] Vinayak Adimule, Basappa C. Yallur, Debdas Bhowmik and Adarsha Haramballi Jagadeesha Gowda. Dielectric Properties of P3BT Doped ZrY_2O_3/CoZrY2O_3 Nanostructure's for Low Cost Optoelectronics Applications. Transaction on Electrical and Electronic Materials. 32 (2021) 12164-12181.

[26] Shashanka Rajendrachari, Bahaddureghatta E. Kumara Swamy, Sathish Reddy, Debasis Chaira, Synthesis of Silver Nanoparticles and their Applications Anal. Bioanal. Electrochem. 5 (2013) 455–466.

[27] R. Shashanka, Volkan Murat YILMAZ, Abdullah Cahit Karaoglanli, Orhan Uzun. Investigation of activation energy and antibacterial activity of CuO nano-rods prepared by Tilia Tomentosa (Ihlamur) leaves. Moroccan Journal of Chemistry. 8, 2 (2020) 497-509.

[28] R. Shashanka, Halil Esgin, Volkan Murat Yilmaz, Yasemin Caglar. Fabrication and characterization of green synthesized ZnO nanoparticle based dye-sensitized solar cell. Journal of Science: Advanced Materials and Devices. 5 (2020) 185-191.

[29] R. Shashanka, B.E. Kumara Swamy. Simultaneous electro-generation and electro-deposition of copper oxide nanoparticles on glassy carbon electrode and its sensor application. S N Applied Sciences. 2(5) (2020) 956.

[30] K.S. Kiran, D. Ramesh, R. Shashanka, Photocatalytic Degradation of Rhodamine B Dye by Nanocomposites: A Review. Applied Mechanics and Materials. 908 (2022) 119-129.

[31] Rayappa Shrinivas Mahale, Shamanth Vasanth, Hemanth Krishna, R. Shashanka, P.C. Sharath, N.V. Sreekanth. Electrochemical Sensor Applications of Nanoparticle Modified Carbon Paste Electrodes to Detect Various Neurotransmitters: A Review. Applied Mechanics and Materials. 908 (2022) 69-88.

[32] Shashanka Rajendrachari, Gururaj Kudur Jayaprakash, Anup Pandith, Abdullah Cahit Karaoglanli1, Orhan Uzun. Electrocatalytic investigation by improving the charge kinetics between carbon electrodes and dopamine using bio-synthesized CuO nanoparticles. Catalysts. 12, 9 (2022) 994.

[33] R. Shashanka, A. C. Karaoglanli, Y. Ceylan, O. Uzun. A fast and robust approach for the green synthesis of spherical Magnetite (Fe_3O_4) nanoparticles by Tilia Tomentosa (Ihlamur) leaves and its antibacterial studies. Pharmaceutical Sciences. 26, 2 (2020) 175-183.

[34] R. Shashanka. Investigation of optical and thermal properties of CuO and ZnO nanoparticles prepared by Crocus Sativus (Saffron) flower extract. Journal of the Iranian Chemical Society. 18, 2 (2021) 415-427.

[35] (a). Adimule Vinayak, Basappa C. Yallur, Vinutha Kamat, and P. Murali Krishna. Characterization studies of novel series of cobalt (II), nickel (II) and copper (II) complexes: DNA binding and antibacterial activity. Journal of Pharmaceutical Investigation. 51, 3 (2021) 347-359. (b). R. Shashanka, Y. Kamacı, R. Taş, Y. Ceylan, A.S. Bülbül, O. Uzun, A.C. Karaoglanli. Antimicrobial investigation of CuO and ZnO nanoparticles prepared by a rapid combustion method. Physical Chemistry Research. 7, 4 (2019) 799-812.

[36] Vinayak Adimule, Basappa C. Yallur, Sheetal Batakurki, Chapter 4 - Design, synthesis, and in vitro anticancer activity of thiophene substituted pyridine derivatives, Recent Developments in the Synthesis and Applications of Pyridines, Elsevier (2023)127-143.

[37] a). R. Shashanka, D. Chaira, B.E. Kumara Swamy. Fabrication of yttria dispersed duplex stainless steel electrode to determine dopamine, ascorbic and uric acid electrochemically by using cyclic voltammetry. International Journal of Scientific & Engineering Research. 7 (2016) 1275-1285. b). R. S. Mahale, R. Shashanka, V. Shamanth, R. Vinaykumar. Voltammetric Determination of Various Food Azo Dyes Using Different Modified Carbon Paste Electrodes. 12 (4) (2022) 4557–4566.

[38] R. Shashanka, B. E. Kumara Swamy. Biosynthesis of silver nanoparticles using leaves of Acacia melanoxylon and its application as dopamine and hydrogen peroxide sensors. Physical Chemistry Research. 8, 1 (2020) 1-18.

[39] R. Shashanka, Kevser Betül Ceylan. The activation energy and antibacterial investigation of spherical Fe_3O_4 nanoparticles prepared by *Crocus sativus* (Saffron) flowers, Biointerface Research in Applied Chemistry. 10, 4 (2020) 5951–5959.

[40] Anik Ü, Timur S, Dursun Z. Metal organic frameworks in electrochemical and optical sensing platforms: a review. Microchimica Acta. 186, 3 (2019) 1-15.

[41] Maalathi Challa, M. R. Ambika, S. R. Usharani, Basappa C. Yallur, Vinayak Adimule. Study on Optical Properties of Cu-MOF Nano Metal Oxide Composites. Applied Mechanics and Materials. 98 (2022) 19-28.

[42] Vinayak Adimule, Sheetal S. Batakurki, Basappa C. Yallur, Rangappa Keri. Enhanced photoluminescence, optical, structural properties of ZrO2-incorporated Sm2O3: Co3O4 nanocomposite and their applications in photocatalytic degradation of methylene blue. Journal of Materials Research. 37 (2022) 2396-2405.

[43] Karmakar A, Prabakaran V, Zhao D, Chua KJ. A review of metal-organic frameworks (MOFs) as energy-efficient desiccants for adsorption driven heat-transformation applications. Applied energy. 269 (2020) 115070.

[44] Gupta N. K, Kim S, Bae J, Kim K. S. Chemisorption of hydrogen sulfide over copper-based metal–organic frameworks: methanol and UV-assisted regeneration. RSC advances. 11, 9 (2021) 4890-4900.

[45] Samuel MS, Savunthari KV, Ethiraj S. Synthesis of a copper (II) metal–organic framework for photocatalytic degradation of rhodamine B dye in water. Environmental Science and Pollution Research. 28, 30 (2021) 40835-40843.

[46] Bauer S, Stock N. Implementation of a Temperature-Gradient Reactor System for High-Throughput Investigation of Phosphonate-Based Inorganic–Organic Hybrid Compounds. Angewandte Chemie International Edition. 46, 36 (2007) 6857-6860.

[47] Iqbal B, Laybourn A, Zaheer M. Size-controlled synthesis of spinel nickel ferrite nanorods by thermal decomposition of a bimetallic Fe/Ni-MOF. Ceramics International. 47, 9 (2021) 12433-12441.

[48] Wu X, Yang C, Ge J. Green synthesis of enzyme/metal-organic framework composites with high stability in protein denaturing solvents. Bioresources and bioprocessing, 4,1 (2017) 1-8.

[49] Dai S, Nouar F, Zhang S, Tissot A, Serre C. One-Step Room-Temperature Synthesis of Metal (IV) Carboxylate Metal-Organic Frameworks. Angewandte Chemie. 133, 8 (2021) 4328-4334.

[50] Kumar Gyanendra, Dhanraj T. Masram. Sustainable synthesis of MOF-5@ GO nanocomposites for efficient removal of rhodamine B from water. ACS omega. 6,14 (2021) 9587-9599.

[51] Ke Fei, Luhuan Wang, Junfa Zhu. Facile fabrication of CdS-metal-organic framework nanocomposites with enhanced visible-light photocatalytic activity for organic transformation. Nano Research, 86 (2015) 1834-1846.